

Wrinkling patterns of thin films under finite membrane strain

Eszter Fehér^{*,**} and András Á. Sipos^{*,**}

^{*}*Department of Mechanics, Materials and Structures,
Budapest University of Technology and Economics, Budapest, Hungary*

&

^{**}*Morphodynamics Research Group,
Hungarian Academy of Sciences – Budapest University of Technology and Economics*

Summary. There is a wide interest in understanding phenomena related to thin and ultrathin surfaces, such as wrinkling, creasing or folding. The classical Föppl-von Kármán plate theory is extensively used to model such phenomena. Significant in-plane strains demand the extension of the classical FvK model. The extended theory predicts the disappearance of wrinkling in the case of rectangular, clamped, stretched sheets, which was verified on thin, polyurethane sheets. In this talk we further develop the model for curved surfaces and present problems, where the extension to the finite tangential strains is essential to investigate the arising wrinkling pattern. By numerical simulation of the governing nonlinear system of PDEs, we investigate the effect of the curvature of the reference configuration on the emerging wrinkling pattern and demonstrate that disappearance of wrinkles takes place on curved surfaces, as well.

1. Introduction

Buckling of thin plates and shells has a rich and inspiring history in solid mechanics. There is a wide interest in wrinkling of thin films recently. In the mechanical point of view, wrinkling itself is a buckling phenomenon, however - opposed to the viewpoint of structural engineering, where buckling should be avoided by any means - now such examples are considered, where postcritical states are acceptable or even desired.

For the study of wrinkling, the Föppl-von Kármán (FvK) theory of thin plates is extensively used, as the small thickness call for taking the effect of the out-of-plane deformations on the in-plane strain tensor into account. Wrinkling of a stretched rectangular sheet clamped at its two opposite edges is widely discussed in the literature [10, 11, 12, 13]. The almost vanishing thickness of the sheet results in a counterintuitive phenomenon, namely wrinkling under dominant tension. Here the two restrained (fixed) edges of the rectangular domain produce a tiny compression, which triggers buckling. The FvK theory properly predicts the appearance of wrinkles for the rectangular sheet, however continuation of the equilibrium path associated with the wrinkled state shows, that the wrinkled pattern is preserved at any value of the applied stretch. On the contrary, extension of the FvK model to the finite in-plane strain regime [1] leads to the conclusion that wrinkles eventually disappear. Experiments on polyurethane sheets [2,3] provided evidence, that disappearance of wrinkles indeed takes place at a critical value of the applied stretch.

Apparently, real-life situations are not restricted to planar problems, in many cases wrinkling occurs on curved surfaces, such as on tents, airbags or biological membranes. In this paper we introduce the extension of the classical FvK shell theory to the finite tangential strain regime. Nevertheless, dependence on the curvature tensor of the reference configuration is introduced into the model. Traditional shell theories treat cases, when the parameterization of the surface is known. For example, one can use cylindrical or polar coordinate systems [8, 15, 16], and the versions of the FvK model are well-known for these parameterizations. The literature of shells is rich in this scope, however, the generalization of these formalism to arbitrary (sufficiently smooth) surfaces is not straightforward.

If one uses the finite element method for the computations, it is natural to present the mechanical model in local coordinates of a coordinate system attached to the \mathbf{n} , outward pointing normal of the surface. In some previous works, the FvK theory was derived using local coordinates to model surfaces having very specific geometries and loads such as the problem of a pinched cylinder. Although in this case an eighth order PDE in the out-of plane deformation component can be derived, the system of governing equations have an appealing form due to the application of the Airy stress function. One can show, that there is no such convenient function for the theory extended to finite tangential strains. On the other hand, it also turns out, that our model can be formulated in an invariant form (i.e. it is independent of the chosen parameterization). Although here we focus on cylindrical surfaces, this feature of the model will trigger applications for more complicated surfaces.

For the numerical work the FEniCS finite element libraries are used [4]. Here we exploit the fact, that the weak form of the governing equations can be applied to define the approximate discrete problem. The new model enables us to investigate the effect of the curvature at the reference configuration on the emerging wrinkling patterns in case of stretched, open cylinders. It is aimed to examine which properties of the wrinkled configuration observed on flat wrinkling sheets preserved on curved surfaces.

2. Wrinkling of a flat, rectangular domain

In our previous work, we treated initially flat, stretched, rectangular films clamped on two opposite sides while the other two sides were left free. The length and the width of the film is denoted by L and W , respectively (Fig. 1. f)).

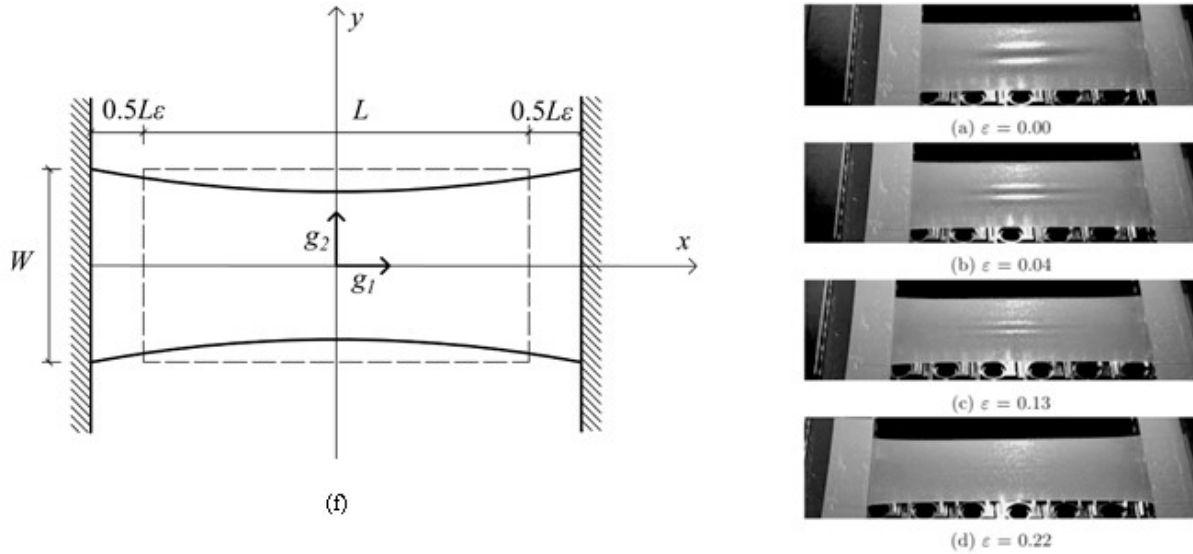


Figure 1: Experimental evidence of disappearance of wrinkles for stretched rectangular sheets, ε denotes the stretch applied between the clamped edges of the pulled sheet. The material is a 40 μm thick polyurethane tape.

We use an orthonormal basis $\{\mathbf{g}_1, \mathbf{g}_2, \mathbf{g}_3\}$, where $\{\mathbf{g}_1, \mathbf{g}_2\}$ span the plane of the film in the reference configuration. The film is assumed to be isotropic, homogeneous and to have a constant thickness h occupying a closed $\Omega \in \mathbb{R}^3$ domain. It is modeled by the deformations of its middle surface $\mathbf{u}_s = [u(x, y), v(x, y)]^T$ denoting the in-plane displacements and $w(x, y)$ is the out-of-plane deformation. According to the FvK theory, the strain energy density is the sum of the membrane (Ψ_m) and the bending (Ψ_b) strain energy densities:

$$\Psi = \Psi_m(\mathbf{E}) + \Psi_b(\mathbf{k})$$

where \mathbf{E} is the Lagrange-Green strain tensor. In the FvK theory the effect of the out-of-plane deformations on the in-plane strain is accounted as

$$\mathbf{E} = \frac{1}{2}(\nabla \mathbf{u}_s + \nabla \mathbf{u}_s^T + \nabla \mathbf{u}_s \nabla \mathbf{u}_s^T + \nabla w \otimes \nabla w).$$

For small transverse displacements (and moderate curvatures at the deformed configuration) \mathbf{k} is the linearized bending strain tensor:

$$\mathbf{k} = -\nabla^2 w.$$

For a Saint-Venant Kirchhoff material, the strain energy densities take the following form:

$$\Psi_m = \frac{Yh}{2(1-\nu^2)} [\nu(\text{tr}\mathbf{E})^2 + (1-\nu)\mathbf{E} \cdot \mathbf{E}],$$

$$\Psi_b = \frac{Yh^3}{24(1-\nu^2)} [\nu(\text{tr}\mathbf{k})^2 + (1-\nu)\mathbf{k} \cdot \mathbf{k}],$$

where Y is the Young-modulus and ν is the Poisson ratio. In the classical theory, infinitesimal strains are assumed, therefore the term $\nabla \mathbf{u}_s \nabla \mathbf{u}_s^T$ in the strain tensor is neglected. In our problem, the surface is loaded by displacements imposed along two sides of its boundary $\partial\Omega_f \subset \partial\Omega$, and the magnitude of that displacements is parameterized by a single parameter ε . The remaining part of the boundary $\partial\Omega \setminus \partial\Omega_f$ is free. As there are no external loads, the total potential energy is simply:

$$I(\mathbf{u}) = \int_{\Omega} \Psi d\Omega$$

After rescaling, the first variation of the energy yields the Euler-Lagrange equilibrium equations:

$$\begin{aligned}\nabla \cdot [(\mathbf{I} + \mathbf{g}_1 \otimes \nabla u + \mathbf{g}_2 \otimes \nabla v)\mathbf{N}] &= \mathbf{0} \\ h^2 \Delta^2 w - \nabla \cdot (\mathbf{N}\nabla w) &= 0\end{aligned}$$

where \mathbf{N} is the Second Piola-Kirchhoff stress associated with the in-plane deformations. We investigate stable solutions of these governing equations (which is verified by the positive definiteness of the second variation of the potential energy in our computations).

It is well-known, that for certain aspect ratios of the rectangle and sufficiently thin films wrinkles appear due to the Poisson-effect and warping at a critical stretch [17]. The extension of the model to finite in-plane strains predicted that wrinkles disappear in a second bifurcation point regardless of the thickness [1]. The classical Föppl-von Kármán plate equations do not hint for such a phenomenon. It was also pointed out, that just some aspect ratios of the domain exhibit wrinkling. These predictions were verified experimentally by displacement controlled pull tests of 28 μm thick polypropylene and 40 μm thick polyurethane sheets [2,3] (Fig. 1. b)). As for the wrinkle crests, it is debated whether the number of wrinkles varies during the stretching process. Nonetheless, in our experiments and numerical simulations we only encountered cases, where the number of the wrinkles were constant. The validity of these characteristics of rectangular sheets is to be analyzed in the presence of curvature of the reference configuration.

3. A model for curved reference configuration

The FvK plate theory was generalized to curved cylindrical surfaces by T. von Kármán himself [8]. Expressing the Navier equations in curvilinear coordinates, one can derive a parameterization-free form for the infinitesimal in-plane strain tensor \mathbf{e} of curved surfaces [7] as

$$\mathbf{e} = \frac{1}{2}(\nabla_X \mathbf{u}_s + \nabla_X \mathbf{u}_s^T) + w\mathbf{K},$$

where $\nabla_X(\cdot)$ denotes the surface gradient operator, \mathbf{u}_s and w are the tangential and normal components of the deformation vector \mathbf{u} , respectively (i.e. $w = \mathbf{u} \cdot \mathbf{n}$ and $\mathbf{u}_s = \mathbf{u} - w\mathbf{n}$). Finally, $\mathbf{K} = \nabla_X \mathbf{n}$ is the curvature tensor, that is a surface gradient of the outward pointing unit vector field \mathbf{n} . With this in hand, for the FvK theory with finite in plane strains the Lagrange-Green strain can be formulated as

$$\mathbf{E} = \frac{1}{2}(\nabla_X \mathbf{u}_s + \nabla_X \mathbf{u}_s^T + \nabla_X \mathbf{u}_s \nabla_X \mathbf{u}_s^T + \nabla_X w \otimes \nabla_X w) + w\mathbf{K}.$$

We keep our assumption about moderate curvatures of the wrinkles, thus the equilibrium equations are derived as

$$\begin{aligned}\nabla_X \cdot [(\mathbf{I} + \nabla_X \mathbf{u}_s)\mathbf{N}] &= \mathbf{0}, \\ h^2 \Delta_X^2 w - \nabla_X \cdot (\mathbf{N}\nabla_X w) + \mathbf{N} \cdot \mathbf{K} &= 0,\end{aligned}$$

where $\Delta_X(\cdot)$ denotes the surface Laplacian. Nevertheless, the model reproduces the equations of the flat case with $\mathbf{K} = \mathbf{0}$, and by eliminating the components of \mathbf{u}_s one can derive the eight-order ODE for w published in Kármán's works.

4. Implementation and validation

From the derivation of the model it is clear, that besides the geometry of the surface in the reference configuration, we also need to know its unit normal vector field. Supposing that it is not known *a-priori*, it can be approximated from the discrete representation of the surface using the coordinates of the finite element nodes. Provided we are able to calculate the surface gradient for arbitrary (smooth) fields given by global coordinates, there is no need to establish a map to define the local coordinate system on the surface.

During the implementation we used our numerical continuation framework implemented in FEniCS [4]. Since the weak form has second order derivatives, we used a discontinuous Galerkin formulation - in specific the interior penalty method - and C_0 continuous finite elements. One of the advantages of FEniCS is that in the case of solving PDEs on manifolds, it naturally computes the surface gradient lying in the tangent plane.

A suitable problem to validate the model is the buckling of thin-walled cylinders. Analytical and numerical results are available for both axially compressed and laterally loaded problems. Furthermore, an axially stretched cylinder loaded by external pressure can be considered as a three-dimensional generalization of the original problem. Wrinkles appear due to the in-plane compression and increasing the stretch leads to the trivial unwrinkled solution gaining back stability. The geometry is simple and the normal vector field can be readily expressed using global coordinates. The

two ends of the cylinder are loaded by prescribing an axial deformation of the boundary. Assuming a constant lateral pressure on the surface, the weak form of the governing equations is:

$$\begin{aligned} & \int_{\Omega} \mathbf{N} \cdot \nabla_x \boldsymbol{\eta}_s dx - \int_{\Omega} \mathbf{N} \cdot \nabla_x \mathbf{n} \zeta dx \\ & + h^2 \int_{\Omega} \Delta_x w_x \zeta dx - \int_{\partial E} \{\Delta_x w\} [\nabla_x \zeta] dS - \int_{\partial E} \{\Delta_x \zeta\} [\nabla_x w] dS + \frac{\alpha}{h_{avg}} \int_{\partial E} \{\Delta_x w\} [\nabla_x \zeta] dS \\ & + \int_{\Omega} \mathbf{N} \nabla_x w \cdot \nabla_x \zeta dx = \int_{\Omega} p \zeta dx, \end{aligned}$$

where $\boldsymbol{\eta}_s, \zeta$ are the tangent and normal components of the test function $\boldsymbol{\eta}$ living in the same function space as \mathbf{u} ; $\{\}, []$ are discontinuous Galerkin operators, α is a penalty parameter and h_{avg} is the average element size. The discontinuous Galerkin terms enforce the required continuity on the ∂E the boundary of an element [18,19].

For validation of the numerical method we considered two benchmark cases.

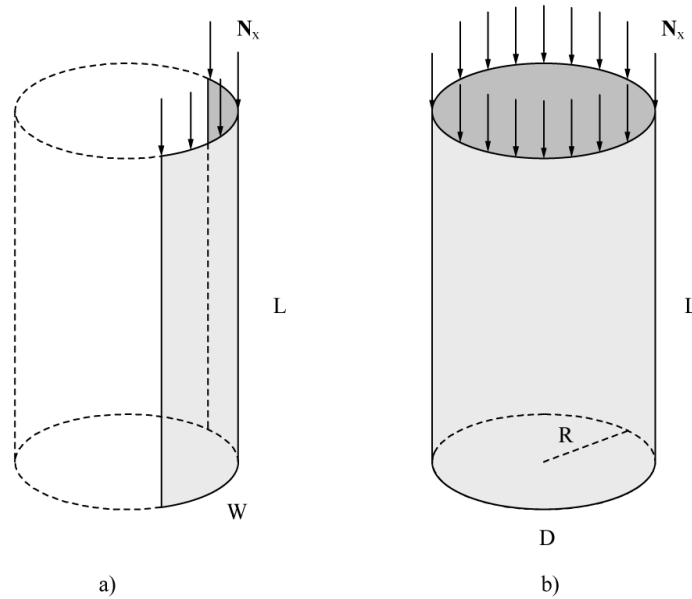


Figure 2: The two cases used for verification of the numerical scheme.

Case-1: buckling of an open cylindrical shell [14]. The critical load in case if compression along the curved, hinged edges (while the other two, straight edges are free) is found to be

$$\sigma_{cr} = \frac{1}{8.11} \left(1 - 0.0146 \frac{\beta}{\pi} \right) \frac{Yh}{R\sqrt{3(1-\nu^2)}}$$

where $0.5\pi \leq \beta \leq \pi$ is the half of the sectorial angle. In Table 1 we compare the stress at the numerical bifurcation of the trivial, unbuckled state to this value.

2β	h	σ_{cr}	σ_{cr}^{comp} 40x80 mesh
π	0.02	0.00021	0.00021
	0.05	0.00052	0.00054
	0.1	0.00103	0.00100
$3/2\pi$	0.02	0.00031	0.00030
	0.05	0.00075	0.00073
	0.1	0.00155	0.00150
$9/5\pi$	0.02	0.00037	0.00035
	0.05	0.00093	0.00085
	0.1	0.00186	0.00155

Table 1: Numerical critical loads of a cylindrical shell with $W=25$, $L=50$, $Y=1$, $\nu = 0.30$ compared to the solution from the literature

Case-2: buckling of a closed cylinder. Using numerical continuation in pressure p and axial deformation ε we determined the bifurcation points where the initially unwrinkled surface buckles. The axial stresses can be computed from the strain tensor:

$$\sigma = \frac{N_x}{h} = \frac{\mathbf{E}[1,1] + \nu(\mathbf{g}_2 \cdot (\mathbf{E}\mathbf{g}_2))}{1 - \nu^2}$$

The analytical solution for a buckling mode determined by n , m the wave numbers circumferentially and axially, respectively derived by Timoshenko [6] for an axially compressed cylinder in case of $p = 0$ is:

$$\sigma_{cr}(n, m) = \frac{S_1}{S_2} \frac{Y}{(1 - \nu^2)},$$

where

$$S_1 = (1 - \nu^2)\lambda^4 + \alpha[(n^2 + \lambda^2)^4 - (2 + \nu)(3 - \nu)\lambda^4 n^2 + 2\lambda^4(1 - \nu^2) - \lambda^2 n^4(7 + \nu) + \lambda^2 n^2(3 + \nu) + n^4 - 2n^6],$$

$$S_2 = \lambda^2 \left\{ (n^2 + \lambda^2)^2 + \frac{2}{1 - \nu} \left(\lambda^2 + \frac{1 - \nu}{2} n^2 \right) [1 + \alpha(n^2 + \lambda^2)^2] - \frac{2\nu^2 \lambda^2}{1 - \nu} + \frac{2\alpha}{1 - \nu} \left(\lambda^2 + \frac{1 - \nu}{2} n^2 \right) [n^2 + (1 - \nu)\lambda^2] \right\},$$

$$\alpha = \frac{h^2}{12R^2},$$

$$\lambda = \frac{mR\pi}{H},$$

here R is the radius and L is the length of the cylinder. The minimum of the equation above for n and m determines the absolute critical value of the compressive stress. In Table 2 we compare the stress at the numerical bifurcation of the trivial, unbuckled state to this value.

h	σ_{cr}	σ_{cr}^{comp} 35x40 mesh	σ_{cr}^{comp} 60x90 mesh
0.025	0.00144	0.00188	0.00167
0.05	0.00288	0.00333	0.00293
0.1	0.00549	0.00061	0.00568

Table 2: Numerical critical loads of the axially compressed column compared to solution of the literature for two different meshes and different thickness values

5. Applications

First, we investigate the effect of the curvature of the reference configuration on the disappearance of the wrinkled pattern. We considered a rectangle with dimensions $L=50$ and $W=25$ curved (and stretched) along its longer edges. For zero curvature the model reproduces the critical stretches associated with the appearance and disappearance of wrinkles of the flat rectangle. Increase in the curvature reduces the distance of the critical points in the stretch direction, for a given thickness of the film there is a critical value of the curvature at which the lower and upper critical values coincide. Above the critical value of the curvature no wrinkles appear regardless of the magnitude of the applied stretch (Fig. 3.).

Second, we determine the stability boundary for stretched, but externally pressurized (perfect) cylindrical shells. We modeled a cylinder with a height $L=40$, $R=10$, and thickness $h = 0.1$ with $\nu = 0.3$ and $Y = 1$. In our computations, (in accordance with the results for the open cylinder in Figure 3), axially stretched cylinders without lateral load (e.g. $p = 0$) do not exhibit wrinkles. The qualitative behavior described in [5] is captured (Figure 4): the critical value of the axial compression is increased by the internal and decreased by the external pressure.

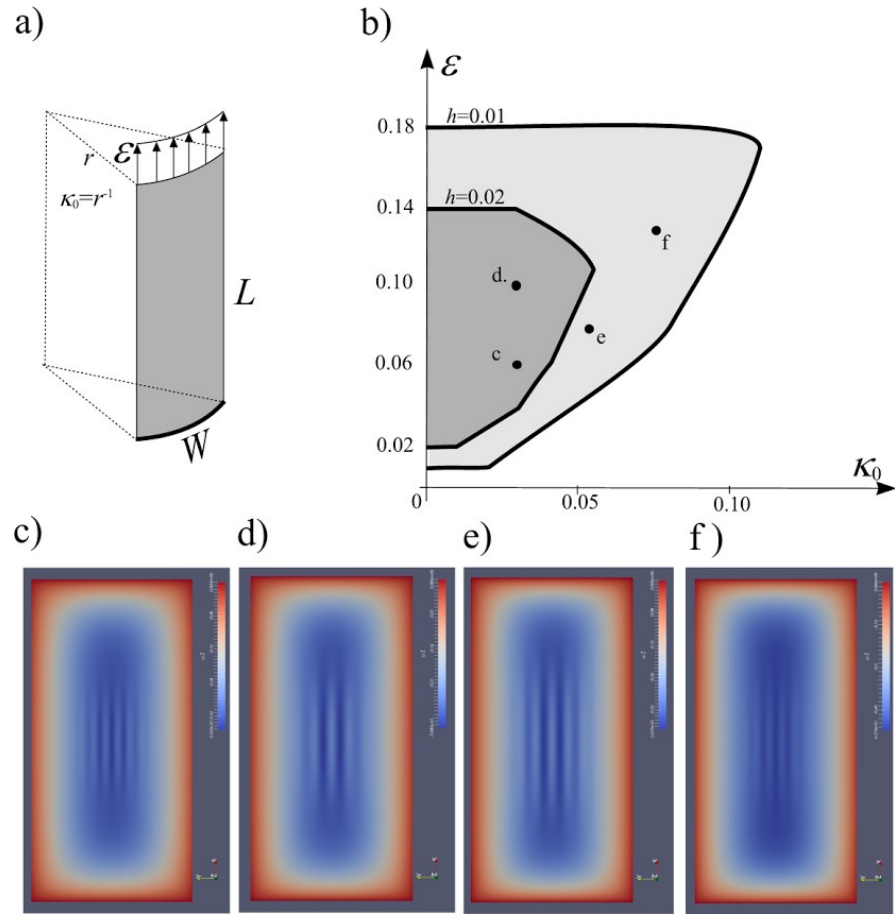


Figure 3: Disappearance of wrinkles for a stretched, open cylinder and the effect of the curvature of the reference state on the critical stretches. a) depicts the cylindrical shell stretched along its curved edges (the other two edges are free). b) critical stretches, where wrinkles appear/disappear for thickness $h=0.01$ and $h=0.02$. In the shaded area the wrinkled configuration is stable. The emerging patterns for several cases are plotted in the c)-e) subfigures. (c: $h=0.02$, $\varepsilon=0.06$, $\kappa_0=0.03$, d: $h=0.02$, $\varepsilon=0.10$, $\kappa_0=0.03$, e: $h=0.01$, $\varepsilon=0.08$, $\kappa_0=0.06$, f: $h=0.01$, $\varepsilon=0.12$, $\kappa_0=0.08$)

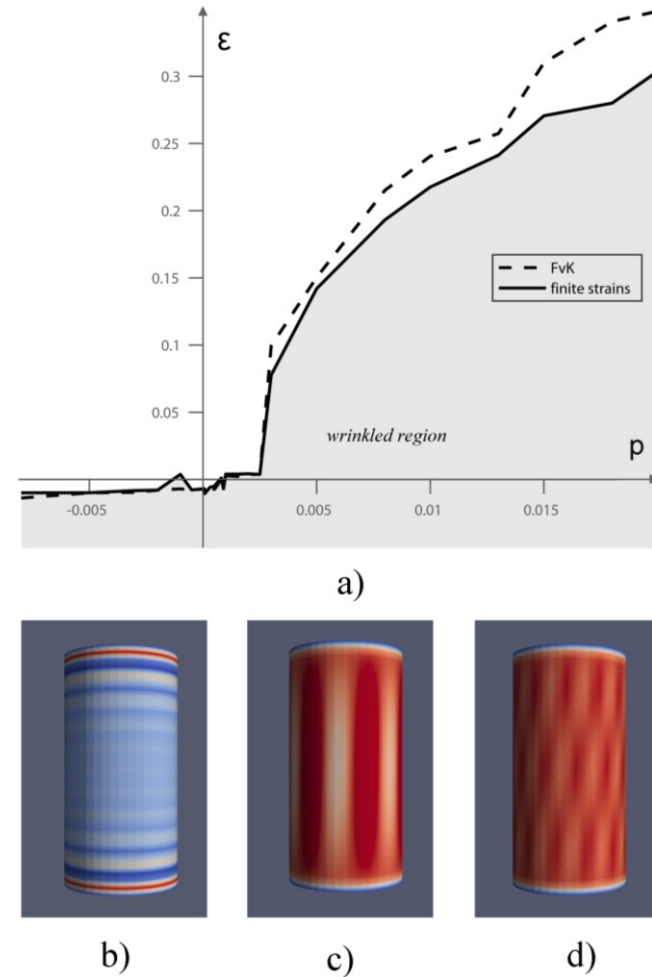


Figure 4: Simultaneous axial and lateral loading of a thin, cylindrical shell. a) is the numerically obtained stability boundary of the problem: observed, that at a fixed external pressure there is a critical stretch, ε which makes the wrinkled pattern disappear. Also note the quantitative difference between the classical FvK and the model extended to finite strains. Wrinkled patterns around the stability boundary b) $p = 0.00008$, c) $p = 0.0009$, d) $p = 0.0025$

5. Conclusions

In this paper the generalization of the classical FvK shell theory for finite tangential strains is introduced. We computationally demonstrate, that the disappearance of wrinkles observed in case of flat, rectangular domains is effected by the curvature of the reference configuration and that for a given thickness there exists a critical value of that curvature, above which there is no wrinkling regardless of the applied stretch. We also showed, that the numerical scheme can be applied for curved surfaces directly. The stability boundary for a stretched and simultaneously externally pressurized cylindrical shell is obtained. Our model does not depend on a specific parameterization of the surface, thus non-conventional curved surfaces will be analyzed in the future.

References

- [1] Healey, T.J., Li, Q., Cheng, R.B., 2013. Wrinkling behaviour of highly stretched rectangular elastic films via parametric global bifurcation. *J. Nonlinear Sci.* **23**:777–805
- [2] Fehér E., Sipos A.A., 2014. Wrinkling of stretched, thin sheets: occurrence and disappearance of the wrinkling pattern. *Építés-Építészettudomány* **42**: 23–42. (in Hungarian)
- [3] Sipos A.A., Fehér E., 2016. Disappearance of stretch-induced wrinkles of thin sheets: a study of orthotropic films. *Int. J. Solids & Struct.* **97-98**: 75-283.
- [4] Logg A., Mardal K-A., Wells G. N. *Automated Solution of Differential Equations by the Finite Element Method: The FEniCS Book*, Springer-Verlag Berlin Heidelberg, 84, 2012.
- [5] Ventsel E., Krauthammer T., 2001. *Thin Plates and Shells. Theory, Analysis, and Applications*. CRC Press, pp. 688.
- [6] Timoshenko S.P., Gere J. M., 1961. *Theory of elastic stability*. McGraw-Hill Book Company, Inc., New York.
- [7] Howell P., Kozyreff G., Ockendon J. 2008. *Applied Solid Mechanics*. Cambridge University Press.
- [8] Karman T., Tsien H. S., 1941. The buckling of thin cylinders under axial compression and bending. *Journ. Aero. Sci.* **8**, No. 8 p. 303.
- [9] Cerda E., Mahadevan L., 2003. Geometry and physics of wrinkling. *Phys. Rev. Lett.* **90**, 1-4.
- [10] Cerda E., Ravi-Chandar K., Mahadevan L., 2002. Wrinkling of an elastic sheet under tension. *Nature* **419**, 579-580.
- [11] Coman C., 2007. On the applicability of tension field theory to a wrinkling instability problem. *Acta Mech.* **190**, 57-72.
- [12] Davidovitch B., Schroll R.D., Vella D., Add-Bedia M., Cerda E., 2011. Prototypical model for tensional wrinkling in thin sheets. *PNAS* **108** (45), 18227-18232.
- [13] Friedl N., Rammerstorfer F., Fischer F., 2000. Buckling of stretched strips. *Comput. Struct.* **78**, 185-190.
- [14] Magnucka-Blandzi E., Magnucki K., 2004. Elastic buckling of an axially compressed open circular cylindrical shell. *Proc. Appl. Math. Mech.* **4**, 546-547.
- [15] Southwell R.V., 1914. On the General Theory of Elastic Stability. *Phil. Trans. R. Soc. Lond.* **A213**, 187-244.
- [16] Donnell L.H., 1933. Stability of thin-walled tubes under torsion. NACA Rep. 479.
- [17] Silvestre N., 2015. Wrinkling of stretched thin sheets: Is restrained poisson's effect the sole cause? *Eng. Struct.* **106**, 195-208.
- [18] Rivière B., 2008. *Discontinuous Galerkin Methods for Solving Elliptic and Parabolic Equations: Theory and Implementation*. SIAM Frontiers in Applied Mathematics
- [19] Brenner S.C., Sung L.Y. 2005. C0 interior penalty methods for fourth order elliptic boundary value problems on polygonal domains. *J. Sci. Comput.* **22**: 83-118.

Acknowledgements

Supported by the ÚNKP-16-3 New National Excellence Program of the Ministry of Human Capacities (FE) and by the János Bolyai Research Scholarship of the Hungarian Academy of Sciences [SA].